Retinoschisin expression and localization in rodent and human pineal and consequences of mouse *RS1* gene knockout

Yuichiro Takada,[1,2] **Robert N. Fariss,**[2] **Morten Müller,**[3] **Ronald A. Bush,**[1,2] **Elisabeth J. Rushing,**[4] **Paul A. Sieving**[1,2]

[1]*National Institute on Deafness and Other Communication Disorders and* [2]*National Eye Institute, National Institutes of Health, Bethesda, MD;* [3]*Institute of Medical Anatomy, Panum Institute, University of Copenhagen, Copenhagen, Denmark;* [4]*Department of Neuropathology and Ophthalmic Pathology, Armed Forces Institute of Pathology, Washington, DC*

Purpose: The pineal gland shares a common neuroectoderm origin with the retina, and like the retina, regulates circadian rhythms through melatonin secretion. Recent expressed tag sequence (EST) analysis showed that several gene mutations, including *RS1*, which cause retinal degeneration, are also expressed in the pineal gland. Mutations in *RS1* result in structural delamination of the neural retinal layers, leading to formation of schisis cavities in men affected with "X-linked retinoschisis" (XLRS). In this study, we evaluated *RS1* expression in the rat and mouse as well as in human pineal and looked for morphological changes in the pineal of the *RS1* knockout (*RS1*-/Y) mouse.
Methods: We analyzed rat and mouse pineal for *RS1* expression by Northern blot and in situ hybridization. RS protein, synaptophysin, S-100, and GFAP localization in the pineal of rat and mouse and RS protein in human pineal were evaluated immunohistochemically. Morphological studies were performed using transmission electron microscopy and light microscopy comparing wild-type to the *RS1*-/Y mouse.
Results: *RS1* expression was detected in RNA isolated from both the pineal and retina as a single major band migrating at about 5.5 kbp in Northern blots. *RS1* riboprobe in situ hybridization demonstrated message in rat and mouse pineal, and immunohistochemistry showed RS protein in pinealocytes expressing synaptophysin but not in interstitial GFAP- and S100-positive glial cells. RS protein was present in many pinealocytes in human pineal. In light and electron microscopic examination of the pineal gland from *RS1*-/Y mice none of the structural changes found in the retina, such as cavity formation and loosening of the tissue, were seen.
Conclusions: This study demonstrates that RS protein is expressed in the pinealocytes but not in interstitial glial cells. The lack of structural abnormalities in the *RS1*-/Y mice suggests that RS serves a different function in the pineal gland than in the retina.

Mammalian retina and pineal gland share several morphologic and physiologic features, including the ability to respond to environmental light. Both organs originate from the neuroectoderm and are developed under common gene regulation [1-3]. Pinealocytes are evolutionarily related to the photoreceptors in the retina [4], and express subgroups of retinal genes including phototransduction molecules [5] that are associated with retinal disease [6,7] EST cluster analysis has shown that the *RS1* is common to both the retina and pineal gene databases [8].

RS1 contains six exons and encodes a 224 amino acid protein, retinoschisin, that contains a highly conserved region called the discoidin domain which appears to function as an adhesion site [9]. Mutations in the *RS1* gene cause X-linked retinoschisis (XLRS) in affected males. XLRS leads to a loosening of the retinal structures with separation and cavity formation in retinal layers that can be imaged in vivo by optical coherence tomography (OCT) [10,11]. The clinical consequences of XLRS include early onset visual impairment, bilateral foveal schisis cavities [12,13], and reduction of the b-

wave amplitude of the electroretinogram (ERG) leading to an electronegative configuration of the ERG waveform [14]. A mouse model of XLRS (*RS1*-/Y) has been made by gene targeting of *RS1*, which shows retinal pathology and the electronegative ERG abnormality similar to that found in XLRS males [15,16]. AAV delivery of the *RS1* gene restores the ERG to a normal configuration in *RS1*-/Y mice [16,17], demonstrating that RS protein plays an important role in synaptic conductivity and retinal structure. Although the pattern of *RS1* expression and the consequences of gene disruption have been surveyed in the retina [18-20], no studies to date have considered *RS1* expression in the pineal gland or possible morphological changes in the *RS1*-/Y mouse. We analyzed rat and mouse pineal gland using RS immunohistochemistry and in situ hybridization and have evaluated the pineal morphology at the light and electron microscopic level in wild-type and *RS1*-/Y mice.

METHODS

Animals and tissue preparation: Twelve adult Sprague-Dawley (SD) rats, ten wild-type (WT) and ten *RS1*-/Y mice [16], all approximately three months of age, were used in this study. Animal handling and the experimental protocol were approved by the NIH Animal Care and Use Committee. Following sac-

Correspondence to: Paul A. Sieving, National Eye Institute, National Institute of Health, 31 Center Drive, Building 31, Room 6A03, MSC 2510, Bethesda, MD, 20892; Phone: (301) 496-2234; FAX: (301) 496-9970; email: paulsieving@nei.nih.gov

rifice with carbon dioxide, rats and mice were perfused transcardially with 4% paraformaldehyde (PFA) in 0.1 M sodium phosphate buffer (PB, pH 7.4) for 10 min. Eyes were removed and fixed in the same fixative for 2 h for in situ hybridization and immunofluorescence, and with 4% glutaraldehyde in 0.1 M PB for 48 h for electron microscopy.

Digoxygenin (DIG) labeled cRNA probe preparation: DIG-labeled cRNA probe was generated (20) using template retinal cDNA containing topoisomerase binding site for RS and β-actin and amplified by PCR using the following primer pairs: RS1-TOPO forward: 5'-CGG AAC AAG GGC AAG CCC CTG GGT TTC GAG TCA-3'; RS1-TOPO reverse: 5'-TGA GTC AAG GGC ACT TGC TGG CAC ACT CAA GCA-3'; β-actin-TOPO forward: 5'-CGG AAC AAG GGT CAT GAA GTG TGA CGT TGA CAT CCG T-3'; β-actin-TOPO reverse: 5'-TGA GTC AAG GGC TTA GAA GCA TTT GCG GTG CAC GAT G-3'. Each template was ligated with T7 (5'-end) or T3 (3'-end) promoter by TOPO element system (Invitrogen) and sub-cloned following instructions. The antisense and sense cRNA probes were synthesized by transcription using T7 (sense) and T3 (antisense) RNA polymerase in the presence of DIG-UTP (Roche, Indianapolis, IN) for 1 h at 37 °C.

Northern hybridization: Total RNA was prepared from pineal and retina using RNeasy (Qiagen, Valencia, CA) and was separated on a formaldehyde-agarose 1% gel, transferred to a nylon membrane (Roche), and probed by hybridizing with DIG-labeled cRNA probe for RS and β-actin at 42 °C. After washing in 2X SSC/0.1% SDS at room temperature for 1 h, and 0.1X SSC/0.1% SDS at 68 °C for 1 h, membranes were incubated with alkaliphosphatase conjugated anti-DIG antibody (Roche), and signal was developed using CDP star (Roche) on Hyper Film (Amersham, Piscataway, NJ).

Immunoblot: Immunoblotting of RS in the pineal gland and the retina of rats was performed using isolated tissue homogenized in 10 volumes of Mammalian Cell Lysis Buffer (Sigma, St. Louis, MO) and centrifuged at 15,000 rpm for 30 min. Protein concentration was determined by the BCA method (Pierce, Rockford, IL). Five micrograms of the protein sample

was fractioned by 12% NuPAGE gel (Invitrogen) and electroblotted onto a nitrocellulose membrane. Blotted membrane was incubated with rabbit polyclonal anti-RS antibody and mouse monoclonal anti-β-actin antibody (Sigma) as the internal control in PBS containing 0.1% Tween-20 and 1% skimmed milk, and visualized with West Pico Detection System (Pierce).

In situ hybridization: In situ hybridization was performed on 5 mm frozen sections from rat pineal. Sections were air-dried and treated sequentially with 0.2 N HCl, 20 μg/ml pro-
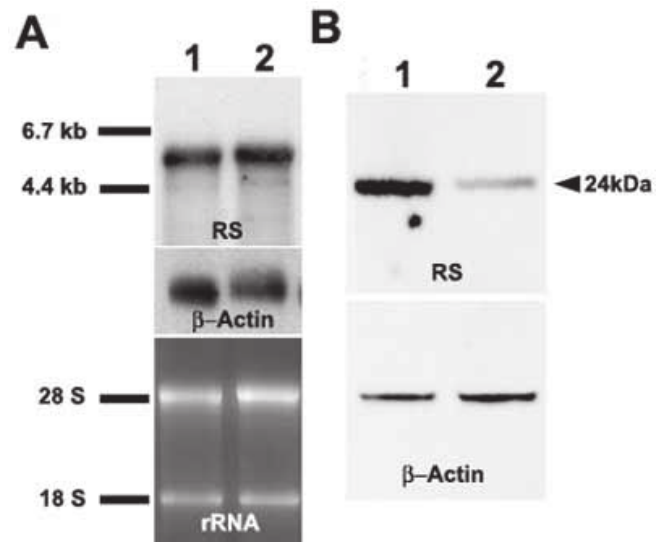

Figure 1. *RS1* message and retinoschisin protein in the rat pineal. **A**: Northern hybridization for *RS1* mRNA from retina (lane 1) and pineal gland (lane 2) was probed with digoxigenin-labeled cRNA probe, with β-actin as control (middle panel). Two bands corresponding to 28S and 18S ribosomal RNA are seen on the ethidium bromide stained agarose gel before transferring to the membranes (lower panel). **B**: Western blot immunolabeling of retinal (lane 1) and pineal (lane 2) fractions with rabbit anti-RS antibody (upper band) and mouse anti β-actin antibody as the loading control (lower band).
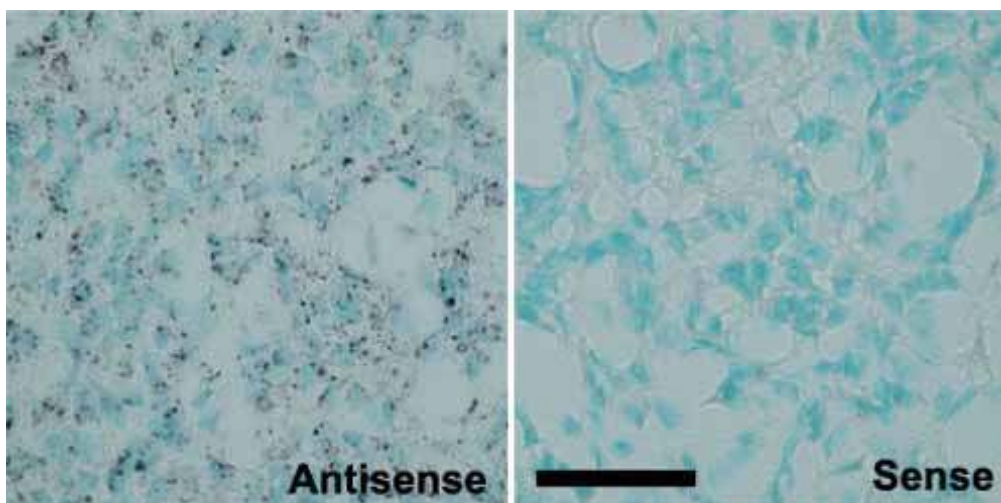

Figure 2. *RS1* message distribution in the rat pineal. In situ hybridization shows *RS1* mRNA in pinealocytes with RS antisense cRNA probe (left) but no signal with the sense probe (right). Scale bar represents 40 μm.

teinase K in 2 mM $CaCl_2$ and 20 mM Tris-HCl buffer (pH 7.5), and acetylated with 0.25% acetic anhydride in 0.1 M triethanolamine (pH 8.0) to prevent nonspecific binding of the probes. The slides were washed with 2X SSC (1X SSC=0.15 M NaCl and 0.015 M sodium citrate) and then prehybridized in a solution containing 50% formamide and 2X SSC at 42 °C for 2 h. Hybridization was performed on slides using a 20 µl mixture containing 50% formamide, 2X

SSC, 1 mg/ml tRNA, 0.5 mg/ml sonicated salmon sperm DNA, 2 mg/ml bovine serum albumin, 10% dextran sulfate, and the cRNA probe (0.2 µg/ml) at 42 °C for 16 h in a moist chamber. The slides were rinsed three times with 2X SSC, 1X SSC, 0.2X SSC, and 0.1X SSC/50% formamide at 50 °C for 15 min each. Immunochemical detection was performed with TSA system (PerkinElmer, Boston, MA), counterstained with methyl green, and observed with a light microscope.
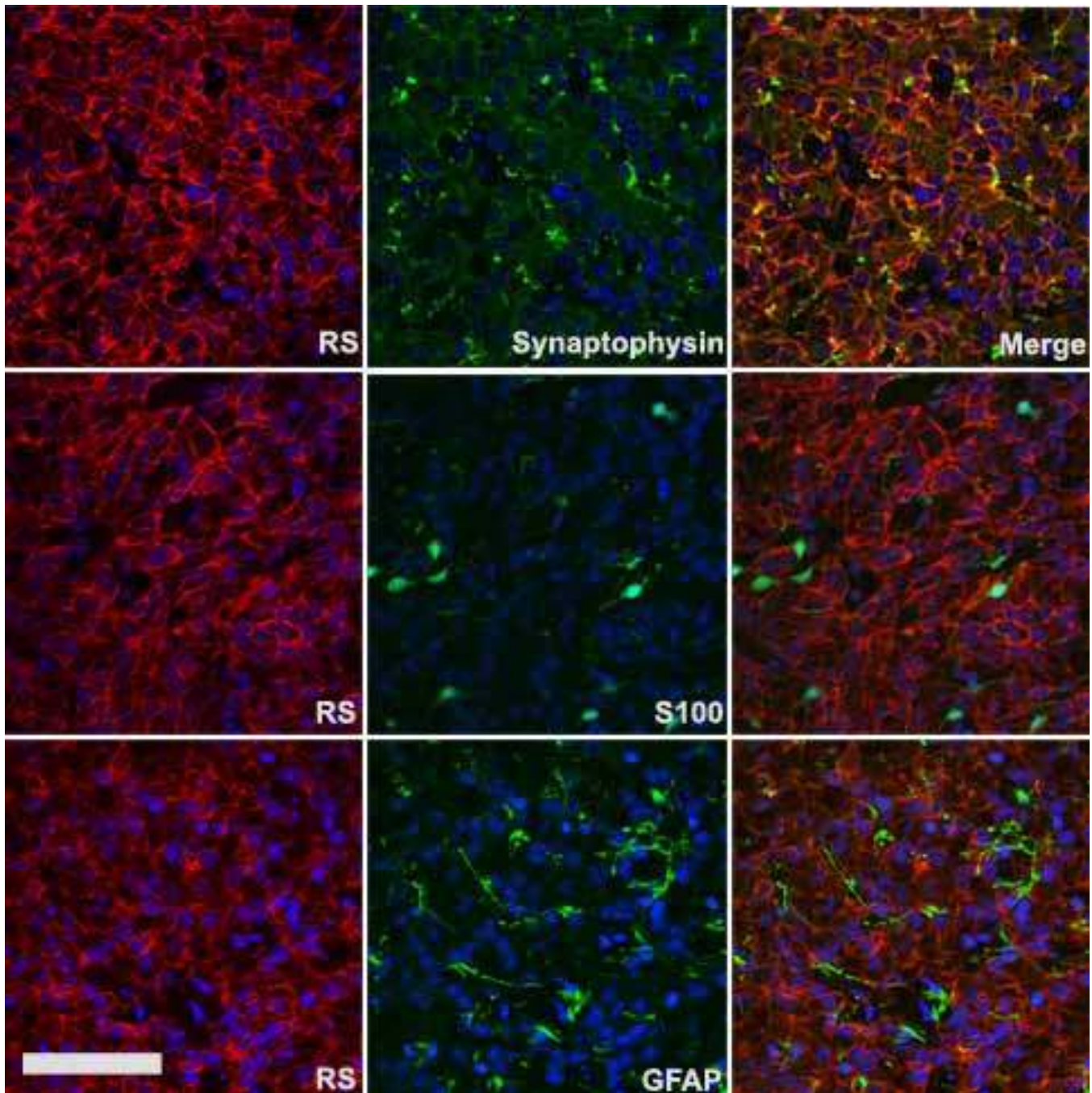

Figure 3. Colocalization of retinoschisin with synaptophysin, S-100, and GFAP in the rat pineal. Immunofluorescence double labeling in the rat pineal with antibodies against retinoschisin (red), synaptophysin (green), S-100 (green), and GFAP (green). A membranous pattern of staining with retinoschisin antibody colocalized with synaptophysin staining in pinealocytes and their synaptic vesicles, but not with S-100 and GFAP in interstitial glial cells. The scale bar represents 75 µm.

Immunohistochemistry: For immunofluorescence, rat and mouse (WT and *RS1*^{-/Y}) pineal sections were blocked in 5% normal goat serum, and then incubated at 4 °C with rabbit anti-RS, mouse anti-synaptophysin (Sigma), S100 (Chemicon) and GFAP (Sigma). Slides were washed in PBS and then incubated for 2 h at room temperature (RT) with Alexa568-conjugated goat anti-rabbit IgG or Alexa488-conjugated goat anti-mouse IgG, with DAPI for nuclear staining. Images were collected using a laser confocal microscope (SP2, Leica). For immunoperoxidase staining of RS protein in a human pineal, paraffin embedded tissue was deparaffinized, washed in PBS and then blocked with 2.5% normal horse serum for 30 min. Sections were incubated with anti-RS antibody overnight followed by a further wash in PBS. Following this sections were incubated with ImmPress horseradish peroxidase conjugated anti-rabbit IgG (Vector laboratory, Burlingame, CA) for 30 min. After a final wash in PBS, color was developed with diaminobenzedene for 15 min and sections were counterstained with methyl green. For negative control, the primary antibody was omitted.

Transmission electron microscopy: Fixed mouse pineal glands were dehydrated in a series of ethanols (30%, 50%, 70%, and 96%), block-stained in 1% uranyl acetate in absolute ethanol for 1 h, rinsed in 2 x absolute ethanol and embedded via propylene oxide in Epon®. Two-μm thick survey sections were cut and counterstained with toluidine blue. Ultrathin sections, with a gray interference color, were cut from preselected areas and poststained in uranyl acetate and lead citrate. The sections were viewed in a Philips 208 electron microscope and photographed on a Kodak Eastman Fine Grain 5302 Film. The negatives were scanned into Adobe Photoshop by use of a Umax PowerLook flat bed scanner at 2400 dpi. The scanned images were resized to 300 dpi, and after density adjustments were montage labeled in Adobe Photoshop.

RESULTS

RS1 *mRNA expression and distribution in the pineal:* Evidence of *RS1* message was explored in rat pineal. Northern hybridization analysis, evaluated using the DIG-labeled *RS1* cRNA probe, demonstrated expression of message in the rat pineal

(Figure 1A). A single major band migrated at about 5.5 kbp in RNA isolated from both the pineal and retina. In situ hybridization for *RS1* mRNA was performed in the rat pineal using the DIG-labeled *RS1* antisense cRNA probe and displayed punctuate signals distributed across the pineal (Figure 2). No specific staining was detected in adjacent sections hybridized with *RS1* sense cRNA.

RS protein expression in the pineal: An immunoblot stained with the RS antibody label showed a single band at 24 kDa in both the retinal and pineal fractions (Figure 1B). No immunoreaction was detected on sections that had been incubated with RS antigen peptides (not shown). Levels of expression were considerably lower in the pineal than in retina. Based on band density, the level of RS protein relative to actin was approximately 10 times higher in retina than in pineal.

Immunolabeling of RS in the pineal: The parenchyma of the pineal gland is composed of pinealocytes and interstitial glial cells. Double labeling immunohistochemistry was performed in pineal with anti-RS and antibodies specific for either neuronal or glial cells (Figure 3). Immunostaining using affinity-purified RS antibody gave a consistent and specific pattern of immunostaining in the pineal. A membranous cellular pattern was seen throughout the pineal with immunofluorescence staining. No immunoreaction was detected in control experiments in rat using antigen-peptide adsorbed RS antibody (data not shown). RS colocalized with both the diffuse synaptophysin labeling of pinealocytes [21] and the scattered punctuate labeling of pinealocyte synaptic-like vesicles. S-100 and GFAP labeling did not colocalize with retinoschisin but gave an intense star-shaped labeling of the cytoplasm of interstitial glial cells [22,23]. In human pineal, RS labeling was detected in many of the cells in the lobules of pineal gland (Figure 4). Cellular structure was not as well maintained in the human tissue as in perfusion fixed rat and mouse pineal and thus it was more difficult to localize immunostaining to cell type or structure (Figure 4). However, RS protein appears to be widely and diffusely associated with cell membrane or cytoplasm as well as more densely localized to structures surrounding the nucleus, perhaps the endoplasmic reticulum.
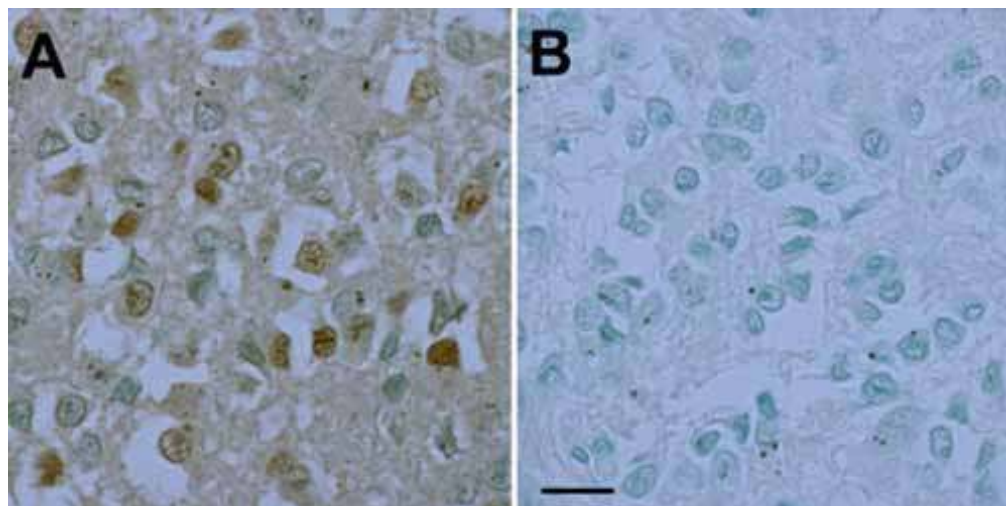

Figure 4. Immunoperoxidase histochemistry in human pineal gland. Immunoreaction of RS was detected in many pineal cells of the lobule (**A**). No immunoreaction was detected in the control slide (**B**). The scale bar represents to 100 μm.
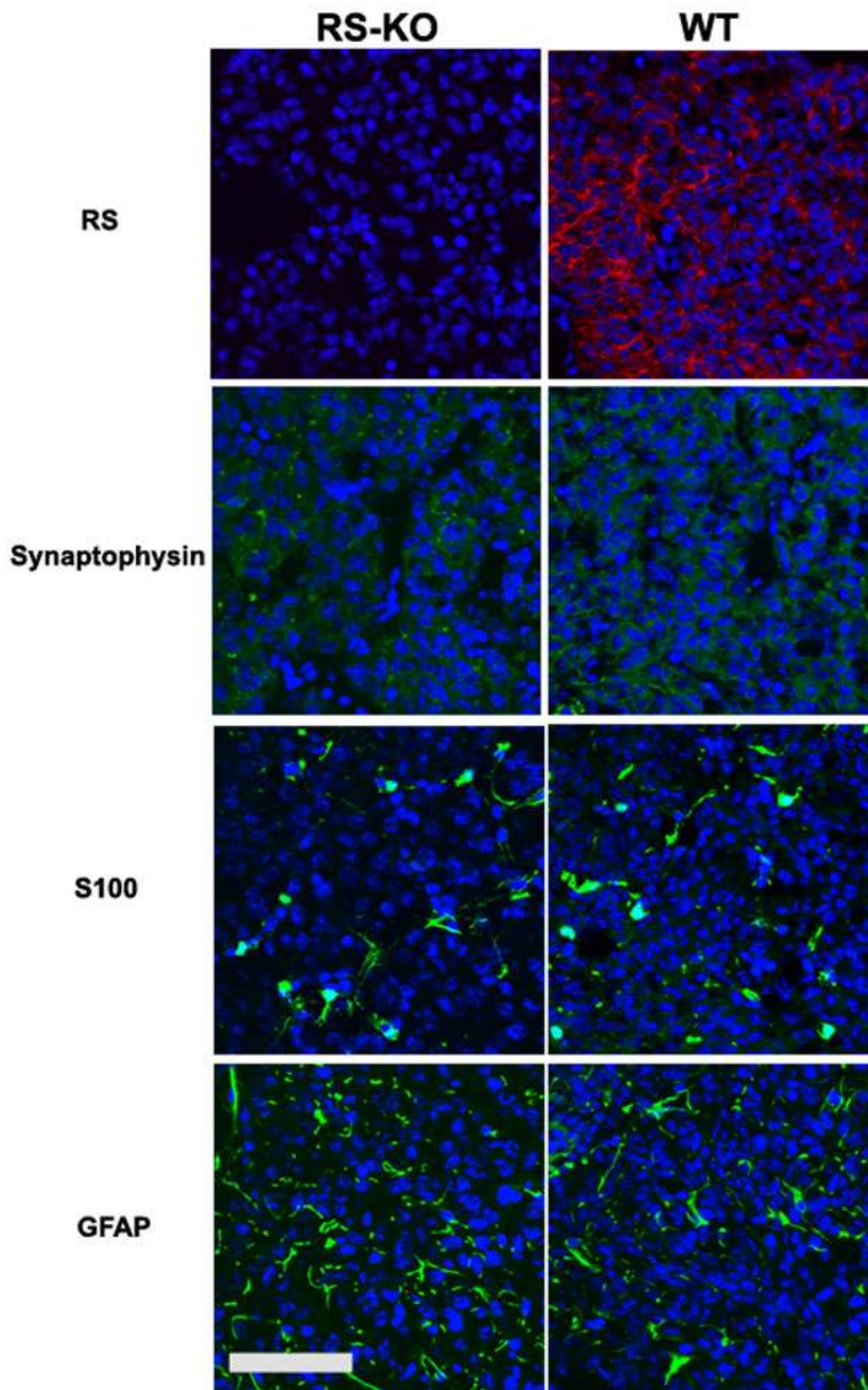
Figure 5. Immunofluorescence labeling in the wildtype and retinoschisin knock-out mouse pineal. Retinoschisin (RS; red signal) immunolabeling showed staining similar to rat in wildtype (WT) pineal, but no immunoreaction was detected in retinoschisin knock-out (RS-KO) pineal. Synaptophysin, S100, and GFAP immunolabeling (green signal) revealed no difference in staining between WT and RS-KO. The scale bar represents 75 μm.

Histological and immunohistochemical evaluation of RS1⁻ᐟY *mouse pineal gland:* Previous histology of the retina of *RS1⁻ᐟY* mouse showed loose organization and intralamellar schisis cavities within the retinal layer structure and prominent reactive glial hypertrophy [15,16]. Retinoschisin was present throughout the pineal of WT mouse, but was not found in the *RS1⁻ᐟY* mouse pineal. Immunolabeling of pineal cell markers, synaptophysin, S100, and GFAP showed no differences between WT and *RS1⁻ᐟY* in amount or distribution of staining (Figure 5).

Electron microscopic analysis: Two μm thick toluidine blue stained survey sections revealed normal pineal morphology in the WT mouse (Figure 6A), with a parenchyma consisting of oval, lightly stained, pinealocytes and triangular darker stained insterstitial cells. The parenchyma was separated by connective tissue spaces with capillaries and perivascular phagocytes. Several myelinated and unmyelinated nerve fibers were observed, both in the perivascular spaces and between the pinealocytes. The *RS1⁻ᐟY* mouse pineal morphology was not different from the wild-type (Figure 6B). At the ultrastructural level the pinealocytes of both the wild-type (Figure 7A,B) and *RS1⁻ᐟY* mouse (Figure 7C,D) contained mitochondria with cristae, Golgi apparatus, rough endoplasmic reticulum, many free ribosomes and several electron lucent and dense core vesicles. The interstitial cells exhibited a darker stained cytoplasm with fewer filaments than observed in the same cells of the rat (not shown).

DISCUSSION

These results indicate that RS message and protein are abundant in the pineal of rat, mouse and human. Double labeling immunohistochemistry demonstrated that RS is expressed in the pinealocytes but not in interstitial glial cells. The absence of RS labeling of pineal glia is mirrored in the retina by the absence of retinoschisin labeling in Müller glial cells [18-20,24]. Colocalization of retinoschisin with synaptic vesicle-like aggregations in pineal is homologous to the association of retinoschisin with synaptic elements in the retina [20,24]. However, in *RS1⁻ᐟY* mice lacking retinoschisin, we found no evidence of pineal morphological changes such as the schisis cavities and delamination seen in the retina of mouse and human XLRS disease. Thus, retinoschisin apparently does not have the same function of maintaining structure in pineal as it does in the retina. This observation is similar to that of other retinal proteins found in the pineal, such as S-antigen, for which the functions are unknown [25,26] (however, see Blackshaw and Snyder [5] and discussion below). The lack of tissue disruption in the pineal in *RS1⁻ᐟY* mice may relate to its structural simplicity, as the pineal does not have the tightly organized layered formation of the retina. Alternatively, other molecules could compensate for the lack of retinoschisin.

The disruption of other genes expressed jointly in the retina and pineal can result in severe retinal degeneration, pineal dysfunction without morphological changes, as well as abnormal circadian rhythms. Disruption of the retinoid-related orphan receptor b (RORb) in mouse causes retinal degeneration and extended circadian cycles in constant darkness, though pineal morphology and light entrainment are normal [27]. Mice with disruption of the cone-rod homeobox gene (*CRX*) show attenuation of circadian entrainment in addition to causing degeneration of retinal photoreceptors and downregulation of several pineal proteins without gross morphological changes [28]. The changes in circadian function in these models of retinal degeneration, however, cannot be definitely linked to changes in the pineal gland function since melatonin, which is the pineal output signal to the circadian system, is not pro-
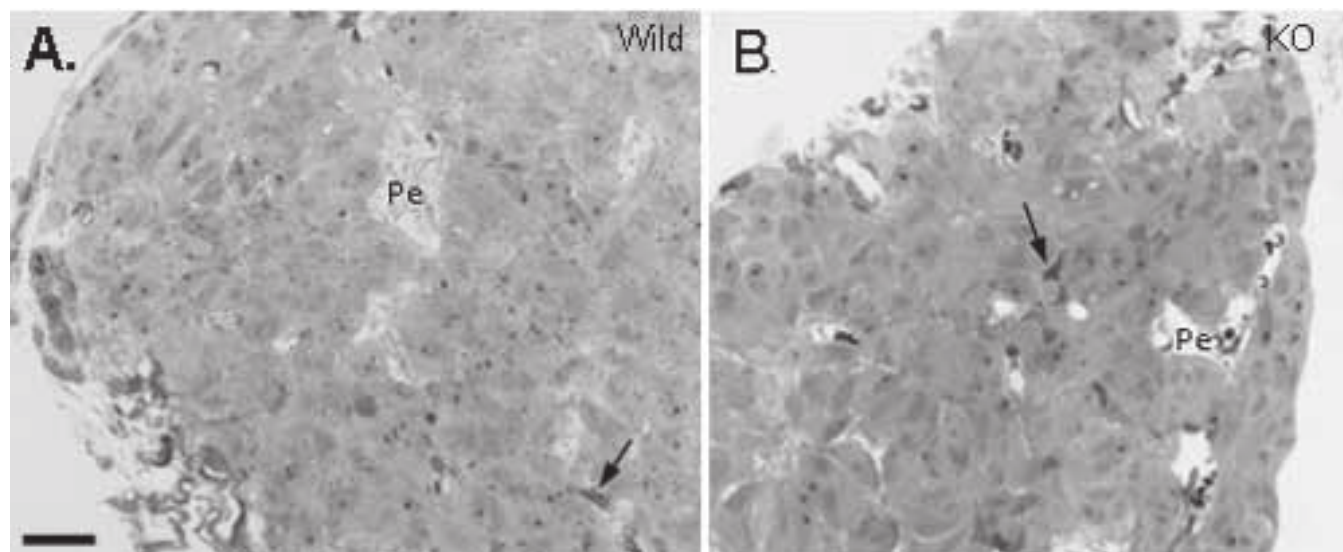

Figure 6. Morphology of WT and RS1-/Y mouse pineal. Epon embedded survey sections 2 μm thick of the pineal gland of WT mouse (**A**) and the RS-KO mouse (**B**). Pineal parenchyma is seen separated by connective tissue spaces with blood vessels and perivascular spaces (Pe). The darker stained interstitial cells (arrows) are seen between the pinealocytes. The scale bar represents 25 μm.

duced in the wild-type background strains used to produce many of the transgenic lines. The circadian effects may be due to the severity of retinal degeneration or to changes in other neurons involved in circadian rhythmicity (e.g., the superchiasmic nucleus [SCN]). In light of the relatively mild visual phenotype seen in patients [12-14] and the limited distribution of retinoschisin in the CNS, *RS1^-/Y* mice would not be expected to exhibit abnormalities in circadian rhythms.

However, it is not known whether the lack of retinoschisin expression during retinal development or the multilayer disruptions of retinal structure occurring in *RS1^-/Y* mice impacts circadian entrainment signaling from specialized melanopsin-containing ganglion cells [29]. No clinical studies to date have reported that XLRS males suffer abnormal sleep patterns that might suggest a disturbance of pineal function.
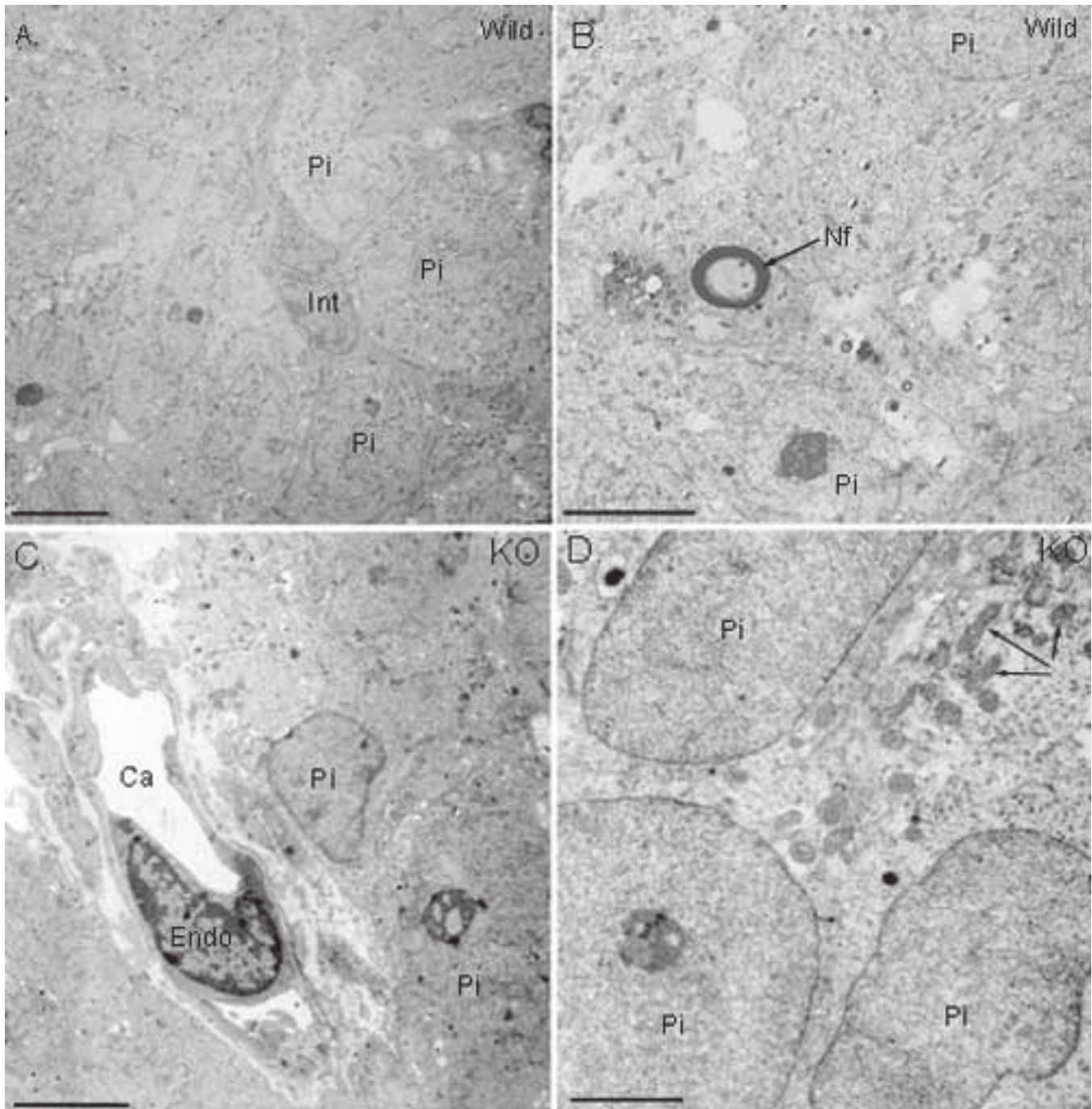

Figure 7. Ultrastructure of WT and RS1-/Y mouse pineal. Electron micrographs showing parts of the superficial pineal gland of the WT mouse (**A**,**B**) and RS-KO mouse (**C**,**D**). Morphology of the knockout mouse pineal is not different from the wild-type mouse. "Int" represents interstitial cell, "Pi" represents pinealocyte, "Endo" represents endothelial cell, "Ca" represents capillary lumen, "Nf" represents myelinated nerve fiber, arrows in Panel **D** indicate mitochondria. The scale bar represents 5 μm in **A**-**C** and 3 μm in **D**.

The *RS1⁻/Y* mouse could be useful in exploring the function of RS in the pineal. However, since these mice do not produce melatonin due to a lack of activity of one of the synthesizing enzymes (hydroxyindole-O-methyltransferase) in the C57BL/6 background strain, it would not be useful to measure melatonin secretion [30,31]. Another avenue would be to investigate the changes in expression of other pineal proteins, such as S-antigen, those involved in indolamine processing or serotonin levels [32]. One reason for investigating S-antigen is a possible functional link between S-antigen and RS at the pinealocyte synapse. In the retina, RS colocalizes with synaptic proteins in the inner and outer retina [20]. This finding, along with its effects on the ERG and loss of structure in synaptic regions of the *RS1⁻/Y* mouse [15,16], suggests it plays a role in synaptic function. As a secreted protein, it could act at the cell membrane between cells to help maintain synaptic structure. In this study, we showed that RS colocalizes with synaptophysin, thus placing it in the regions of the pinealocyte synapse. A role for S-antigen in synaptic function of pinealocytes has also been postulated. It involves the turning off of the G-protein coupled b-adrenergic receptor after phosphorylation, analogous to the interaction of arrestin (S-antigen) with G-protein coupled rhodopsin in the retina [32]. This idea is based on the fact that S-antigen, in sufficient quantities, can take over the function of β-adrenergic arrestin [33]. Since we observed no morphological changes at the ultrastructural level, a structural role for RS affecting function at the pinealocyte synapse is less certain than in the retina. However, in future studies it would be interesting to explore the effects of RS gene knockout on the expression of proteins, such as S-antigen, which might be involved in pineal function.

Pinealocytes are known to express several retinal antigens, including S-antigen, which may be used to clinically characterize the neoplasms that arise from these cells known as pineal parenchymal tumors (PPTs) [34,35]. According to current World Health Organization (WHO) criteria, PPTs are classified as pineocytoma, pineoblastoma and pineal parenchymal tumor with intermediate differentiation [36]. These three classes of pineal tumors have different clinical outcomes for which the histological characterization is an independent prognostic factor by multivariate analysis [37-39] and is based primarily on routine morphologic criteria, particularly mitotic activity. While there is currently no correlation with biomarkers and outcome, identification of biomarkers that may represent potential therapeutic targets or that may facilitate differential diagnosis is an important goal. The present results of pineal immunolabeling indicate that retinoschisin expression in the human pineal is widespread. Because of its abundance, it may offer advantages as a pinealocyte tumor marker compared with S-antigen, which is found in approximately 5-10% of the normal human pinealocytes [26]. Unlike some retinal genes expressed in the pineal which diminish with age and the onset of sympathetic innervation of pineal during development [5], our results show that RS can be detected in the mature pineal gland. We propose that it would be warranted to explore retinoschisin as a pinealocyte cell marker in diagnosing PPTs. Additional studies are needed to determine whether there is a correlation with clinical outcome.

Vector-based gene transfer has been suggested as a therapeutic option for human XLRS disease [16,17]. Of particular concern is that, even with administration of AAV into the closed space of the eye, the gene construct may spread into the brain along the optic nerve or through systemic circulation [40]. The present study shows that the pineal gland is a site of *RS1* expression outside the eye and may raise questions of the consequence of aberrant *RS1* expression following introduction of an AAV-*RS1* construct. Results of our study diminish such concerns as retinoschisin expression in pineal appears to have no morphological consequence, though its effect on function remains to be explored.

REFERENCES

1. Foster RG, Hankins M, Lucas RJ, Jenkins A, Munoz M, Thompson S, Appleford JM, Bellingham J. Non-rod, non-cone photoreception in rodents and teleost fish. Novartis Found Symp 2003; 253:3-23; discussion 23-30,52-5,102-9.
2. Vigh B, Manzano MJ, Zadori A, Frank CL, Lukats A, Rohlich P, Szel A, David C. Nonvisual photoreceptors of the deep brain, pineal organs and retina. Histol Histopathol 2002; 17:555-90.
3. Ekstrom P, Meissl H. Evolution of photosensory pineal organs in new light: the fate of neuroendocrine photoreceptors. Philos Trans R Soc Lond B Biol Sci 2003; 358:1679-700.
4. Klein DC. The 2004 Aschoff/Pittendrigh lecture: Theory of the origin of the pineal gland—a tale of conflict and resolution. J Biol Rhythms 2004; 19:264-79.
5. Blackshaw S, Snyder SH. Developmental expression pattern of phototransduction components in mammalian pineal implies a light-sensing function. J Neurosci 1997; 17:8074-82.
6. Lev S. Molecular aspects of retinal degenerative diseases. Cell Mol Neurobiol 2001; 21:575-89.
7. Hims MM, Diager SP, Inglehearn CF. Retinitis pigmentosa: genes, proteins and prospects. Dev Ophthalmol 2003; 37:109-25.
8. Sohocki MM, Malone KA, Sullivan LS, Daiger SP. Localization of retina/pineal-expressed sequences: identification of novel candidate genes for inherited retinal disorders. Genomics 1999; 58:29-33.
9. Sauer CG, Gehrig A, Warneke-Wittstock R, Marquardt A, Ewing CC, Gibson A, Lorenz B, Jurklies B, Weber BH. Positional cloning of the gene associated with X-linked juvenile retinoschisis. Nat Genet 1997; 17:164-70.
10. Muscat S, Fahad B, Parks S, Keating D. Optical coherence tomography and multifocal electroretinography of X-linked juvenile retinoschisis. Eye 2001; 15:796-9.
11. Azzolini C, Pierro L, Codenotti M, Brancato R. OCT images and surgery of juvenile Macular retinoschisis. Eur J Ophthalmol 1997; 7:196-200.

12. Falcone PM, Brockhurst RJ. X-chromosome-linked juvenile retinoschisis: clinical aspects and genetics. Int Ophthalmol Clin 1993; 33:193-202.

13. George ND, Yates JR, Moore AT. X linked retinoschisis. Br J Ophthalmol 1995; 79:697-702.

14. Peachey NS, Fishman GA, Derlacki DJ, Brigell MG. Psychophysical and electroretinographic findings in X-linked juvenile retinoschisis. Arch Ophthalmol 1987; 105:513-6.

15. Weber BH, Schrewe H, Molday LL, Gehrig A, White KL, Seeliger MW, Jaissle GB, Friedburg C, Tamm E, Molday RS. Inactivation of the murine X-linked juvenile retinoschisis gene, Rs1h, suggests a role of retinoschisin in retinal cell layer organization and synaptic structure. Proc Natl Acad Sci U S A 2002; 99:6222-7.

16. Zeng Y, Takada Y, Kjellstrom S, Hiriyanna K, Tanikawa A, Wawrousek E, Smaoui N, Caruso R, Bush RA, Sieving PA. RS-1 Gene Delivery to an Adult Rs1h Knockout Mouse Model Restores ERG b-Wave with Reversal of the Electronegative Waveform of X-Linked Retinoschisis. Invest Ophthalmol Vis Sci 2004; 45:3279-85.

17. Min SH, Molday LL, Seeliger MW, Dinculescu A, Timmers AM, Janssen A, Tonagel F, Tanimoto N, Weber BH, Molday RS, Hauswirth WW. Prolonged recovery of retinal structure/function after gene therapy in an Rs1h-deficient mouse model of x-linked juvenile retinoschisis. Mol Ther 2005; 12:644-51.

18. Grayson C, Reid SN, Ellis JA, Rutherford A, Sowden JC, Yates JR, Farber DB, Trump D. Retinoschisin, the X-linked retinoschisis protein, is a secreted photoreceptor protein, and is expressed and released by Weri-Rb1 cells. Hum Mol Genet 2000; 9:1873-9.

19. Reid SN, Akhmedov NB, Piriev NI, Kozak CA, Danciger M, Farber DB. The mouse X-linked juvenile retinoschisis cDNA: expression in photoreceptors. Gene 1999; 227:257-66.

20. Takada Y, Fariss RN, Tanikawa A, Zeng Y, Carper D, Bush R, Sieving PA. A retinal neuronal developmental wave of retinoschisin expression begins in ganglion cells during layer formation. Invest Ophthalmol Vis Sci 2004; 45:3302-12.

21. Redecker P, Bargsten G. Synaptophysin—a common constituent of presumptive secretory microvesicles in the mammalian pinealocyte: a study of rat and gerbil pineal glands. J Neurosci Res 1993; 34:79-96.

22. Higley HR, McNulty JA, Rowden G. Glial fibrillary acidic protein and S-100 protein in pineal supportive cells: an electron microscopic study. Brain Res 1984; 304:117-20.

23. Moller M, Ingild A, Bock E. Immunohistochemical demonstration of S-100 protein and GFA protein in interstitial cells of rat pineal gland. Brain Res 1978; 140:1-13.

24. Molday LL, Hicks D, Sauer CG, Weber BH, Molday RS. Expression of X-linked retinoschisis protein RS1 in photoreceptor and bipolar cells. Invest Ophthalmol Vis Sci 2001; 42:816-25.

25. Korf HW, Moller M, Gery I, Zigler JS, Klein DC. Immunocytochemical demonstration of retinal S-antigen in the pineal organ of four mammalian species. Cell Tissue Res 1985; 239:81-5.

26. Huang SK, Klein DC, Korf HW. Immunocytochemical demonstration of rod-opsin, S-antigen, and neuron-specific proteins in the human pineal gland. Cell Tissue Res 1992; 267:493-8.

27. Andre E, Conquet F, Steinmayr M, Stratton SC, Porciatti V, Becker-Andre M. Disruption of retinoid-related orphan receptor beta changes circadian behavior, causes retinal degeneration and leads to vacillans phenotype in mice. EMBO J 1998; 17:3867-77.

28. Furukawa T, Morrow EM, Li T, Davis FC, Cepko CL. Retinopathy and attenuated circadian entrainment in Crx-deficient mice. Nat Genet 1999; 23:466-70.

29. Panda S, Sato TK, Castrucci AM, Rollag MD, DeGrip WJ, Hogenesch JB, Provencio I, Kay SA. Melanopsin (Opn4) requirement for normal light-induced circadian phase shifting. Science 2002; 298:2213-6.

30. Ebihara S, Marks T, Hudson DJ, Menaker M. Genetic control of melatonin synthesis in the pineal gland of the mouse. Science 1986; 231:491-3.

31. Goto M, Oshima I, Tomita T, Ebihara S. Melatonin content of the pineal gland in different mouse strains. J Pineal Res 1989; 7:195-204.

32. Brednow K, Korf HW. Morphological and immunocytochemical features of the pineal organ of C3H and C57BL mice at different stages of postnatal development. Cell Tissue Res 1998; 292:521-30.

33. Benovic JL, Kuhn H, Weyand I, Codina J, Caron MG, Lefkowitz RJ. Functional desensitization of the isolated beta-adrenergic receptor by the beta-adrenergic receptor kinase: potential role of an analog of the retinal protein arrestin (48-kDa protein). Proc Natl Acad Sci U S A 1987; 84:8879-82.

34. Perentes E, Rubinstein LJ, Herman MM, Donoso LA. S-antigen immunoreactivity in human pineal glands and pineal parenchymal tumors. A monoclonal antibody study. Acta Neuropathol (Berl) 1986; 71:224-7.

35. Korf HW, Klein DC, Zigler JS, Gery I, Schachenmayr W. S-antigen-like immunoreactivity in a human pineocytoma. Acta Neuropathol (Berl) 1986; 69:165-7.

36. Mena H NY, Jouvet A, Scheithauer BW. Pineoblastoma. In: Kleihues P, Cavenee WK, editors. Pathology and genetics of tumours of the nervous system. Lyon: IARC Press; 2000. p. 115-122.

37. Fauchon F, Jouvet A, Paquis P, Saint-Pierre G, Mottolese C, Ben Hassel M, Chauveinc L, Sichez JP, Philippon J, Schlienger M, Bouffet E. Parenchymal pineal tumors: a clinicopathological study of 76 cases. Int J Radiat Oncol Biol Phys 2000; 46:959-68.

38. Jouvet A, Saint-Pierre G, Fauchon F, Privat K, Bouffet E, Ruchoux MM, Chauveinc L, Fevre-Montange M. Pineal parenchymal tumors: a correlation of histological features with prognosis in 66 cases. Brain Pathol 2000; 10:49-60.

39. Lutterbach J, Fauchon F, Schild SE, Chang SM, Pagenstecher A, Volk B, Ostertag C, Momm F, Jouvet A. Malignant pineal parenchymal tumors in adult patients: patterns of care and prognostic factors. Neurosurgery 2002; 51:44-55; discussion 55-6.

40. Dudus L, Anand V, Acland GM, Chen SJ, Wilson JM, Fisher KJ, Maguire AM, Bennett J. Persistent transgene product in retina, optic nerve and brain after intraocular injection of rAAV. Vision Res 1999; 39:2545-53.